Asian Journal of Chemistry; Vol. 36, No. 1 (2024), 239-246

ASIAN JOURNAL OF CHEMISTRY

https://doi.org/10.14233/ajchem.2024.30305

Green Mediated Synthesis of Zinc Oxide Nanoparticles using Tamarind Bark Extract and their Applications in Textile Dye Degradation and Antimicrobial Studies

BASKAR GINGIGUNTLA[1], ABIRAMI AKKINIRAJ CHANDRASEKAR[1] and SEBASTIAN ANTONY SELVAN CRUZ[2,*]

[1]Department of Chemistry, Government Arts College for Men, Nandanam, Chennai-600035, India
[2]Department of Chemistry, R.V. Government Arts College, Chengalpettu-603001, India

*Corresponding author: E-mail: csas1966@gmail.com

Received: 17 October 2023; *Accepted*: 16 December 2023; *Published online*: 31 December 2023; AJC-21509

ZnO nanoparticles were synthesized using tamarind bark extract as a green reducing agent in alkaline medium. The tamarind bark solution acts both as a stabilizing and a reducing agent which regulates the size and the shape of the green synthesized zinc oxide nanoparticles. The progressive growth of ZnO nanoparticles was monitored by using UV-visible spectral studies. A sharp peak at 349 nm indicates the formation of spherical shaped zinc oxide nanoparticles. The size and shape of the ZnO nanoparticles were observed using scanning electron microscopy (SEM). The catalytic behaviour of a ZnO nanoparticle was studied for the degradation of textile dyes like methylene blue and Congo red and observed that the degradation reaction follows pseudo first-order kinetics with a rate constant k = 0.0331 min^{-1}, 0.0283 min^{-1} and 0.1175 min^{-1}, 0.1167 min^{-1}, respectively for ZnO nanoparticles at 50 µg and 100 µg. The antimicrobial activity of ZnO nanoparticles was also tested for various Gram-positive, Gram-negative bacteria and fungi in which higher zone of inhibition was observed for Gram-negative microorganism.

Keywords: Nanoparticles, Tamarind bark, Photocatalytic activity, Bactericidal activity, Fungicidal activity.

INTRODUCTION

In 21st century, nanotechnology is found to be a progressive technology which could bring revolution in almost every scientific field. Due to their different size and morphology they have been applied in wide range of applications [1-3]. Among the nanomaterials, metal oxide nanoparticles received a considerable attention due to their size tunable properties, high stability, better photo stability and a wide range of radiational absorption which is due to the high fraction of atoms, at a low cost, easy availability and also in limited toxicity [4-8].

Among the various metal oxide nanoparticles like copper oxide, tungsten oxide, tin oxide, titanium oxide and zinc oxide nanoparticles is found to be in the interest of various researches worldwide due to their versatile and unique chemical, physical, biological and optical properties [9-13]. Because of these properties ZnO nanoparticles finds its application in various fields like optical, electrical, mechanical, biomedical, drug, electrochemical sensing, gas sensing, photocatalyst, wound healing, bio-imaging, *etc*. [14-18]. Many different methods have been used to the synthesize ZnO nanoparticles *e.g*. sol gel method, hydrothermal method, precipitation method, mechanochemical method and green synthesis method [19-24]. Among all these methods green synthesis method is found to be the one of the best cost-effective and eco-friendly method and results in the synthesis of non-toxic nanoparticles for human therapeutic use [25].

Green synthesis of ZnO nanoparticles has been carried out with the extracts of different parts of the plant such as an orange peel extract [26], tamarind pulp extract [27], ginger (*Z. offcinale*) [28], garlic (*Allium sativum*) [29], coffee [30], Aloe vera [31] extract, neem (*Azadirachta idica*) [32], hibiscus (*Hibiscus rosa-sinensis*) extract [33], cardamom [34], *Cayratia pedata* leaf extract [35], *etc*. We are the first to describe ZnO nanoparticle production utilizing tamarind bark extract. The tamarind barks are rich in polyphenols, tannin and other natural compounds. Due to these compounds, tamarind have better antioxidant and anti-inflammatory properties. Moreover, tamarind bark are used in wound healing, anticancer therapy, diabetes, as an effective astringent and can also be used to protect against heart diseases [36,37].

The importance of this work is to study the catalytic property and antimicrobial property of the synthesized ZnO nanoparticles towards the degradation of different textile dyes and various microbes. For health care and environmental system, this microbial and toxic chemical pollution has become a great threat and a need to be created for their eradication. Hence, the progress in developing efficient materials that possess both photocatalytic and antibacterial properties is of significant importance. Since ZnO nanoparticles are superior bactericides that successfully inhibit both Gram-positive and Gram-negative bacteria [38], they have surpassed all other produced metallic nanoparticles, including TiO_2 NPs, Au NPs and Ag NPs [39-41]. On comparing with rod shaped ZnO, the spherical shaped ZnO can release Zn^{2+} ions with much ease and this small sized particles are more permeable to the bacteria membranes [42] and their broad UV absorption spectrum, high exciton binding energy (60 meV), high thermal conductivity, high chemical stability, inertness, high electron mobility and wide band gap 3.2-3.4 eV acts as a better photocatalyst and this can be recycled with lesser degradation in its activity [43,44]. The only drawback is the synthesis process, size and shape control process as it requires toxic chemicals. Hence, a time and cost effective non-toxic green method has been developed for the mass production of size and shape controlled ZnO nanoparticles.

EXPERIMENTAL

Tamarind bark was collected from the campus of Government Arts College, Chennai, India. Zinc sulphate, sodium hydroxide and all other analytical grade chemicals were purchased from SRL chemicals, Chennai, India. Ultrapure water (18.2 MΩ resistance) (Millipore Corp.) was used for the preparation of all the solutions. All the chemicals used as received from the commercial sources.

Characterization: The UV-Visible absorption spectrum was recorded at a room temperature using Shimadzu UV-visible spectrophotometer (model UV1800) dual-beam spectrometer operated at a resolution of 2 nm. The structural and morphology of ZnO nanoparticle was studied using field emission scanning electron microscopy (FE-SEM, SU6600, Hitachi, Japan). The elemental composition of the ZnO nanoparticle was calculated from energy dispersive X-ray spectrometer (EDAX, 8121-H, Japan). The XRD pattern of the powdered sample was analyzed with X′PERT-PRO diffractometer with a Cu$K\alpha$ radiation (λ = 1.5406 Å). To identify the possible functional groups involved in the synthesis of ZnO nanoparticles, the FTIR analysis (Thermo-Fisher Scientific FTIR spectrometer (Nicolet iS10, Madison, USA) was performed using KBr pellet in the range of 4000-500 cm^{-1}.

Tamarind bark extract: Fresh barks were washed several times with running tap water to remove the dust and dirt particles and then washed thoroughly with distilled water. The cleaned barks were allowed to dry in shade for 7 days. Then, the tamarind bark powder was prepared by crushing the bark in an electrical grinder. About 10 g of tamarind bark powder was dissolved in 250 mL of ultrapure water and introduced into the Soxhlet apparatus for 3 h. Then the extract was collected in Erlenmeyer flask and kept in dark until further use.

Green synthesis of ZnO nanoparticles: A 50 mL of tamarind bark extract (pH 12) was taken in an Erlenmeyer flask, an equal amount of zinc sulphate (0.1 M) solution was added dropwise at room temperature. After 12 h, the solution of colour turned from dark brown to reddish brown indicating the formation of ZnO nanoparticle and their formation was further confirmed by recording their absorbance using UV-spectrophotometer. The solution was centrifuged, filtered and dried in an air oven for 1 h. The filtrate was kept in the muffle furnace at 450 ºC for 3 h. The resulting ZnO nanoparticles were preserved in an air tight vial until further use.

Catalytic degradation: The catalytic degradation of textile dyes like Congo red (CR) and methylene blue (MB) using ZnO nanoparticles in an aqueous $NaBH_4$ solution followed by setting up in a standard quartz cell (1 cm path length; 3 mL volume). Then, 0.1 mL of 0.3 M of $NaBH_4$ solution was added to 2.4 mL of 0.1 mM of dye solution solution at 293 K. Upon addition of ZnO nanoparticles (40 µg), the decrease in the absorbance value was recorded by using Shimadzu UV 1800 spectrophotometer at 293 K.

Antimicrobial activity

Agar disc diffusion method: Antimicrobial activity of ZnO nanoparticles was determined by disc diffusion method on Muller-Hinton agar (MHA) medium. Muller-Hinton agar (MHA) medium was poured into the petri-plate and allowed to equilibrate for few minutes and solidification. After the medium was solidified, the inoculums were spread on the solid plates with sterile swab moistened with the microbial suspension. The discs were placed in MHA plates and added 20 µL of sample (conc. of 50, 75 and 100 µg/mL) were placed on the disc. The plates were incubated at 37 ºC for 24 h and then the antimicrobial activity was determined by measuring the zone of inhibition.

RESULTS AND DISCUSSION

Green synthesis of ZnO nanoparticles using tamarind bark extract: Tamarind bark extract was collected and used as green reducing agent for the synthesis of ZnO nanoparticles. Tannins, a polyphenol, present in the tamarind bark extract acts as a reducing agent and found to be responsible for the reduction of metal salt into metal oxide nanoparticle. A colour change of zinc sulphate from colourless solution to brownish red precipitate on adding the extract at pH 12 shows the reduction of metal salts. Fig. 1A UV-graph depicts the formation of zinc oxide at 349 nm and the extract peak at 230 nm. The possible reaction mechanism is shown in **Scheme-I**. On the addition to the bark extract, the Zn^{2+} reacts with the polyphenol and zinc hydroxide is formed with calcination yields ZnO nanoparticles.

Effect of tamarind bark concentration and effect of pH: Tamarind bark extract (pH 12) taken in different volumes (0.1, 0.25, 0.5, 0.75 and 1 mL) and the metal precursor was kept constant as 1 mL and used for the synthesis of ZnO nanoparticles. While increasing the concentration of extract, the SPR (surface plasmon resonance) peak height also increases, which is shown in Fig. 1B. A complete reduction is found for ZnO, which is formed with 1:1 ratio. On further increase of the extract, no

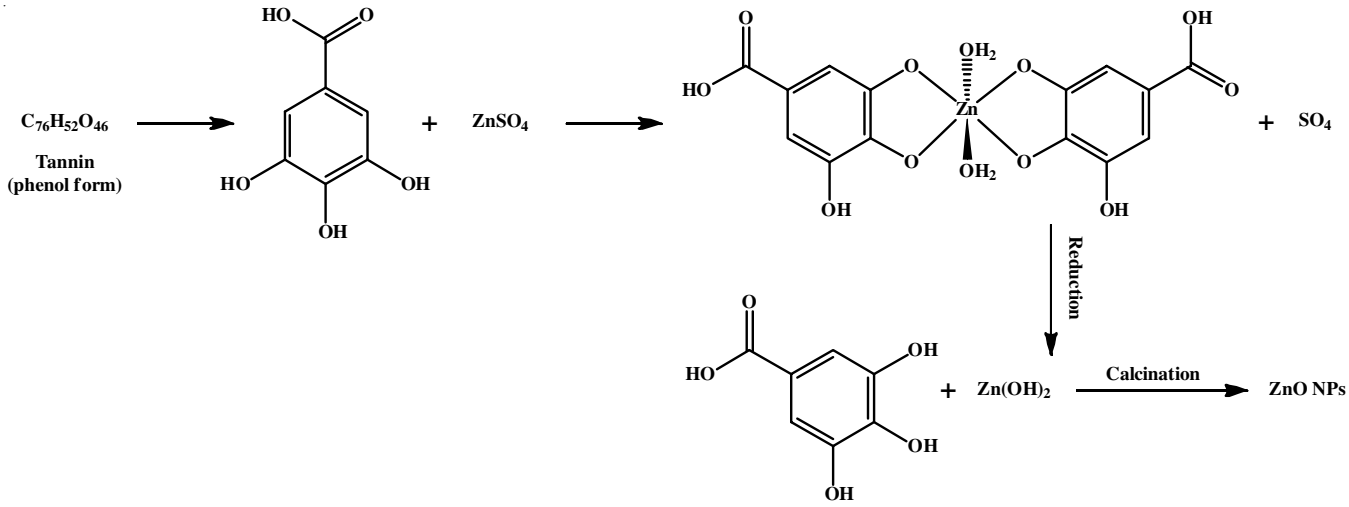

Scheme-I: Reaction mechanism of formation of ZnO nanoparticles

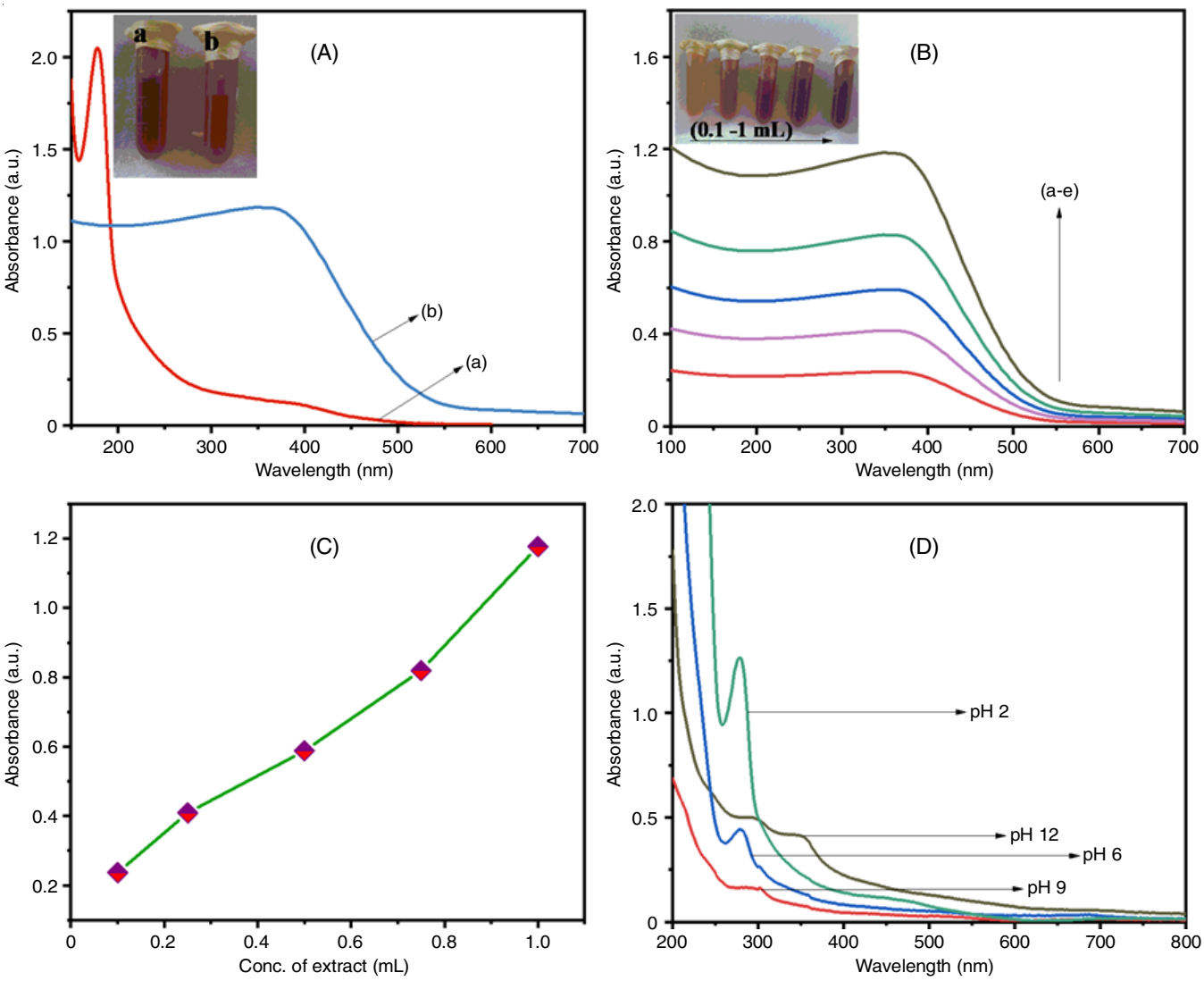

Fig. 1. UV-Vis spectra: Optimization and formation of ZnO nanoparticles using tamarind bark extract (Insert: figure shows the colour formation of ZnO and tamarind bark extract) (A); UV-vis spectra of ZnO synthesized from different tamarind bark extract concentrations (B), plot of λ_{max} values against volume of extract showing red shift with increase in the concentration of extract (C), UV-vis spectra of ZnO nanoparticles synthesized from tamarind bark extract at different pH levels (2, 6, 9 and 12) (D)

further increase in the absorbance peak is found which shows that the complete reduction has taken place. The band gap energy was calculated using E_g = 1240 λeV and found to be 3.75 eV, which is comparable to the energy band gap for ZnO nanoparticles. Fig. 1C graph shows the plot drawn on various concentration of the extract against absorbance of ZnO nanoparticles formed, whereas Fig. 1D shows the influence of pH of extract on the synthesis of ZnO nanoparticles. It is inferred that no absorbance value is found until pH 12 and also the plasmon band position reached the maximum. Hence, pH 12 was chosen as optimum for the synthesis of ZnO nanoparticles.

Structural and morphological characterization of synthesized ZnONPs: The diffraction peaks were observed at 2θ values of 31.753º, 34.415º, 36.238º, 47.535º, 56.576º, 62.845º, 67.935º and 69.040º corresponding to lattice planes (100), (002), (101), (102), (110), (103), (200), (112) and (201) respectively and indicated that the synthesized ZnO NPs are identical to the hexagonal phase of zinc oxide (Fig. 2). These peaks were in good agreement with the reported literature and well consistent with the JCPDS file No. 89-1397.

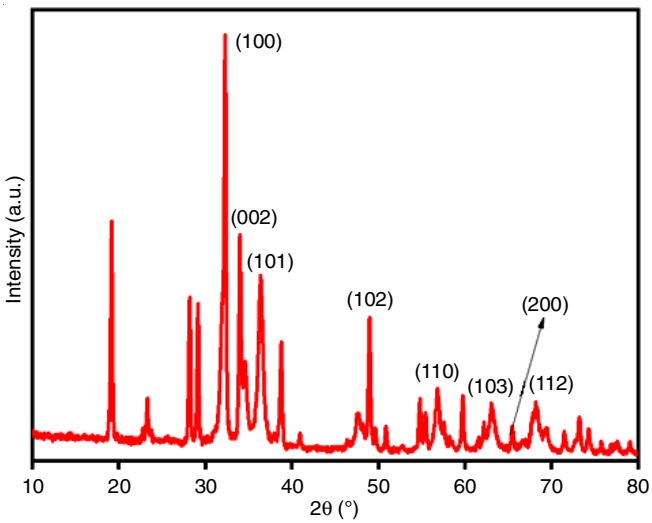

Fig. 2. XRD analysis of ZnO nanoparticles using tamarind bark extract

From the FT-IR spectrum (Fig. 3), it is inferred that reduction of metal precursor is due to the flavonoid and polyphenols present in the extract. The peaks observed at 3516.2 and 3469.2 cm^{-1} are due to O-H stretching vibration, whereas a peak at 3348 cm^{-1} is due to N-H bond. The bands at 1640 and 1115 cm^{-1} shows the presence of C=O and C-C-O groups. A main absorbance band at 617.6 cm^{-1} indicates the presence of C-Br stretching, whereas the band at 435.8 cm^{-1} is due to the presence of Zn-O vibration.

FE-SEM analysis is done at different magnifications to examine the exact size and shape of the synthesized ZnO nanoparticles. The surface morphology confirms the formation of nanoparticles at a semispherical shape in an agglomerated state (Fig. 4a-c). This clearly shows that the particles present in a homogeneous form and the homogeniety of nanoparticles plays an important role in their different activities. The particle size ranges from 58.0 to 80.39 nm and the increase in the size is due to the overlapping of nanoparticles.

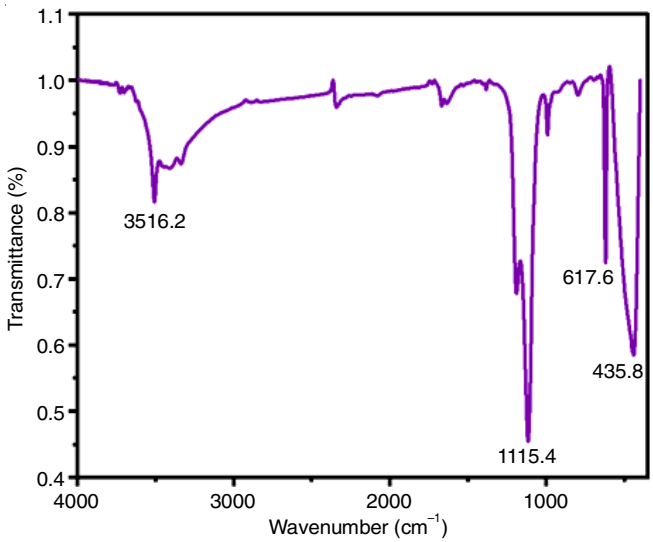

Fig. 3. FT-IR spectrum of ZnO nanoparticles formed using tamarind bark extract

Fig. 4d shows the EDAX pattern of the synthesized ZnO nanoparticles, which revealed a high signal for zinc at 1 eV and 8.5 eV, for oxygen at 0.5 eV confirming the presence of zinc in its oxide form. The weight percentage of Zn and O was found to be 72.94% and 27.06%. Thus, the purity of synthesized nanoparticle is confirmed from the EDAX studies.

Catalytic degradation of textile dyes using synthesized ZnO NPs: To investigate the photocatalytic activity of synthesized ZnO nanoparticles, the photocatalytic degradation of cationic and anionic dyes (methylene blue and Congo red) were performed using ZnO nanoparticles under UV light irradiation. The potocatalytic performance of ZnO against methylene blue and Congo red dyes are shown in Figs. 5 and 6. No significant changes were found in the concentration of methylene blue and Congo red dyes under UV irradiation in the absence of catalysts, indicating that both dyes are stable in aqueous medium under room temperature.

When ZnO catalyst is present, an adsorption phenomenon occurs as a result of the interaction between the negative charges on the surface of catalyst caused by the plant extract and the dyes. The catalytic reductions of dyes were carried out in the presence of $NaBH_4$ and ZnO nanoparticles as catalyst. Though the degradation of dyes is possible with $NaBH_4$ without catalyst, but it is kinetically limited [45]. The UV-absorbance of methylene blue dye exhibit two absorbance peaks, one at 292 nm due to the benzene ring and the other at 664 nm due to the heteropolyaromatic linkage. The peak at 664 nm is considered as the main peak and the absorption intensity of the methylene blue decreases rapidly with the time and the colour of the solution changes from blue to colourless. The breakdown of methylene blue dye took 28 min in the presence of 50 µg of ZnO nanoparticles, but when the catalyst was increased to 100 µg, the degradation was completed in 12 min (Fig. 5a-b).

In case of Congo red (CR) dye, the two predominant peaks were also observed at 500 nm and 340 nm in the UV-spectra , which is attributed due to the N=N and –C-C- groups, respectively. In the same manner as observed in methylene blue, a significant decrease in the absorption value was also observed

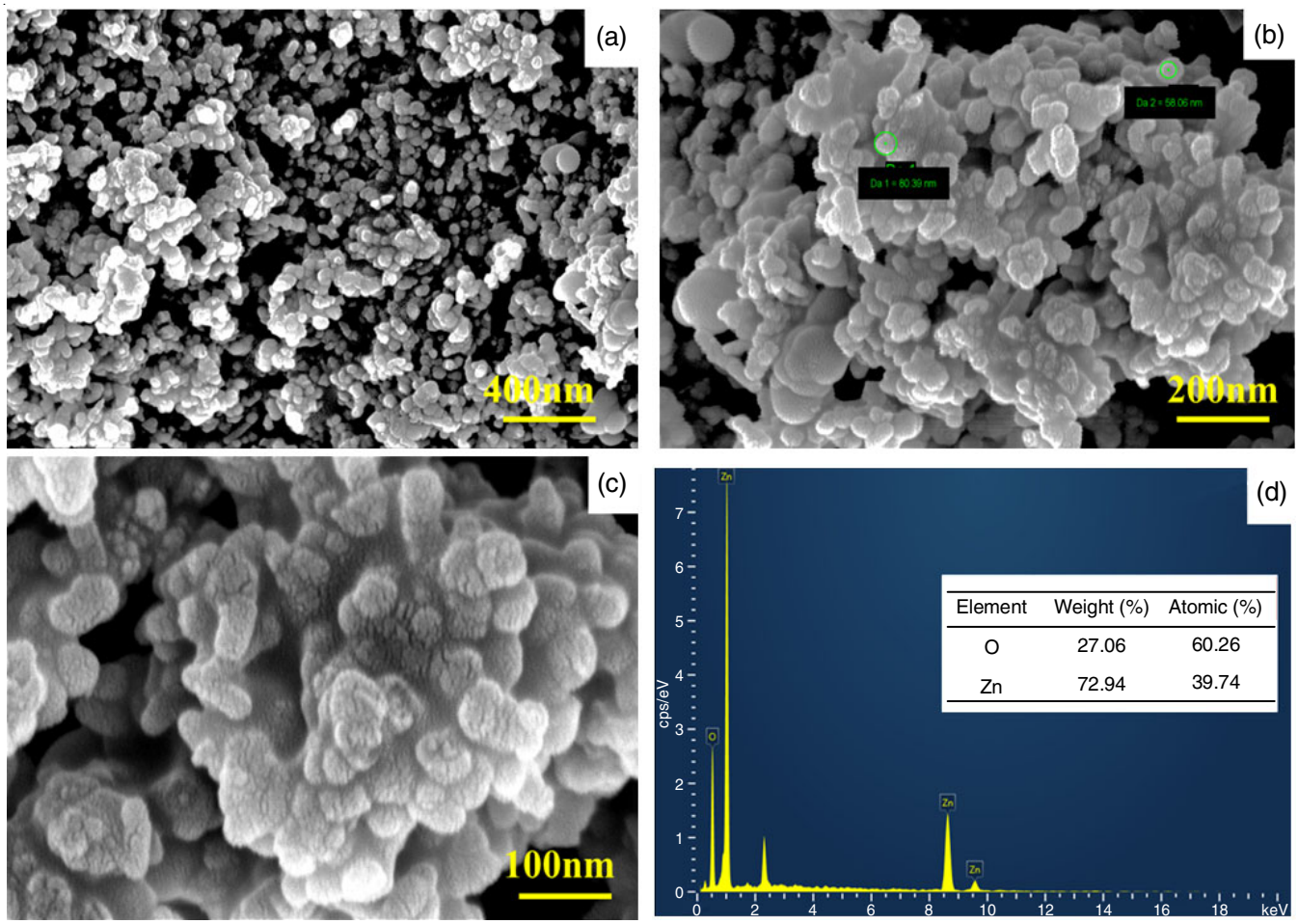

Fig. 4. HR-SEM images of tamarind bark extract synthesized ZnO nanoparticles in different magnifications (a-c) and EDAX spectrum (d)

upon the addition of ZnO catalyst at two different concentrations. ZnO nanoparticles breakdown of Congo red takes 26 min with 50 µg, however with 100 µg catalyst, it can be accomplished in 12 min (Fig. 6a-b).

Both the studied dyes degradation were found to follow pseudo first-order kinetic reaction, which were determined from the slope of plot $\ln(C_o-C_t/C_t)$ *vs.* time. The calculated rate constant for the photocatalytic degradation of methylene blue (Fig. 5c-d) and Congo red (Fig. 6c-d) dyes were k = 0.0331 min^{-1}, 0.0283 min^{-1} and 0.1175 min^{-1}, 0.1167 min^{-1}, respectively for ZnO nanoparticles at 50 µg and 100 µg. From the percentage degradation plot, it was found that ZnO nanoparticles degraded 97% of methylene blue and 93% of Congo red dyes. Thus, it is confirmed that the tamarind bark extract assisted green synthesized ZnO nanoparticles can be used for degradation of toxic pollutants in the environment.

Antimicrobial activity: The antibactericidal activity of synthesized ZnO nanoparticles from tamarind bark extract was tested against various bacterial and fungal organisms. From Table-1, it was found that the all the studied microorganism shows an efficient minimum inhibitory concentrations (MIC) at four different concentrations (25, 50, 75 and 100 µL) of synthesized ZnO nanoparticles. It is confirmed that synthesized nanoparticles shows greater activity towards both bacterial as well as *Candida albicans* fungi organism.

Conclusion

This study presents a straightforward, cost-effective, and environmental friendly approach for synthesizing ZnO nanoparticles from tamarind bark extract. The prepared ZnO nanoparticles were in spherical shape and the particle size ranges from 58.0 to 80.39 nm as confirmed from the SEM studies. The crystalline nature, purity of ZnO and the formation of ZnO nanoparticle were further confirmed by XRD, EDAX, FT-IR and UV studies. Further the prepared ZnO nanoparticles were employed in the catalytic degradation off textile dyes, which gives better results with 97% and 93% of catalytic degradation for methylene blue and Congo red dyes, respectively. The green synthesized ZnO nanoparticles also shows the higher antimicrobial activity against bacterial and fungal organisms.

CONFLICT OF INTEREST

The authors declare that there is no conflict of interests regarding the publication of this article.

REFERENCES

1. G.M. Whitesides, *Small*, **1**, 172 (2005); https://doi.org/10.1002/smll.200400130
2. B. Pelaz, S. Jaber, D.J. de Aberasturi, V. Wulf, T. Aida, J.M. de la Fuente, J. Feldmann, H.E. Gaub, L. Josephson, C.R. Kagan, N.A. Kotov, L.M. Liz-Marzán, H. Mattoussi, P. Mulvaney, C.B. Murray, A.L. Rogach,

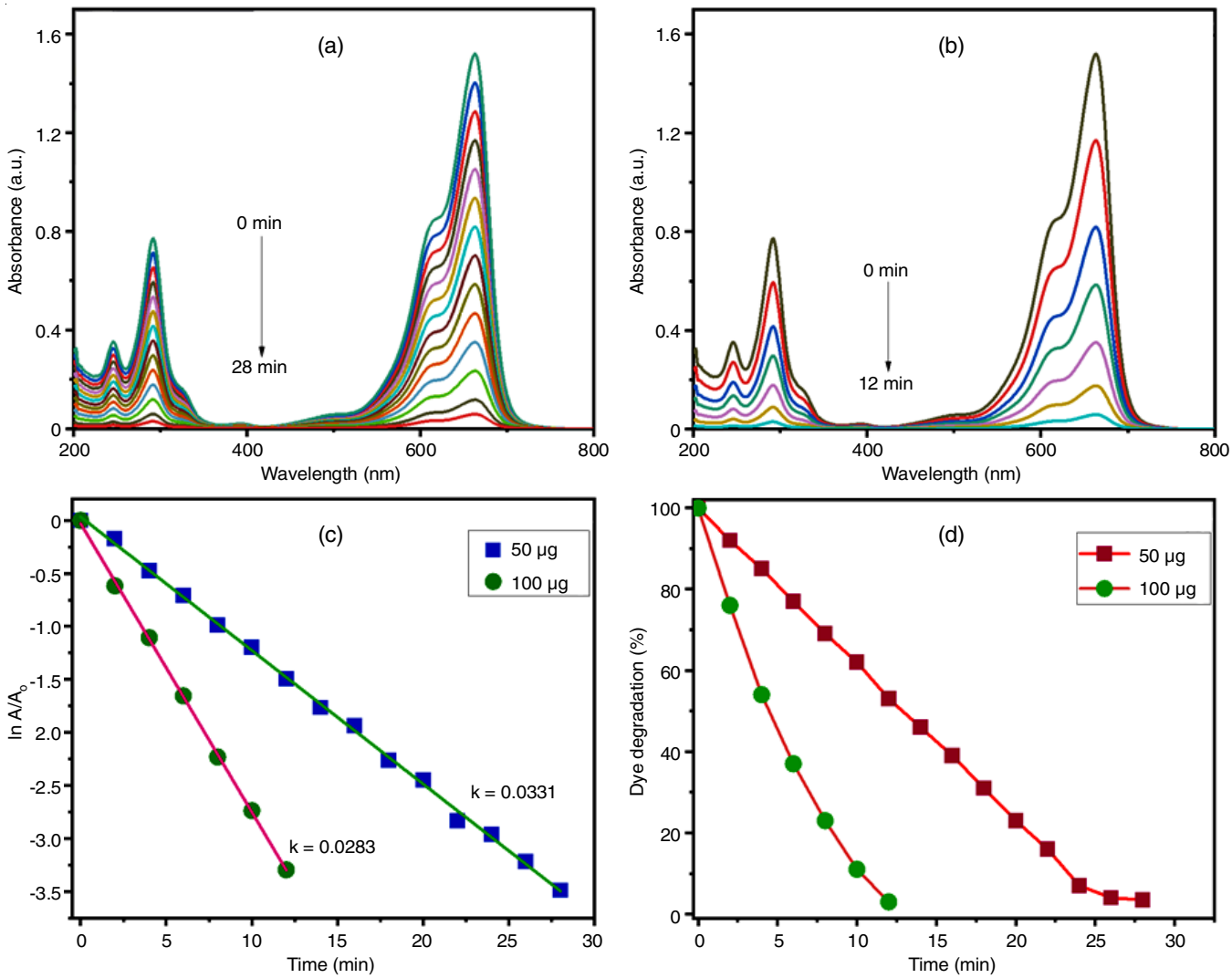

Fig. 5. Time-dependent UV-vis spectra for the catalytic degradation of methylene blue dyes by $NaBH_4$ in the presence of ZnO nanoparticles as catalyst. Conditions: [$NaBH_4$] = 0.3 M; methylene blue = 0.1 mM; ZnO NPs (50 and 100 µg)

P.S. Weiss, I. Willner and W.J. Parak, *ACS Nano*, **6**, 8468 (2012); https://doi.org/10.1021/nn303929a

3. I. Khan, K. Saeed and I. Khan, *Arab. J. Chem.*, **12**, 908 (2019); https://doi.org/10.1016/j.arabjc.2017.05.011
4. W.T. Liu, *J. Biosci. Bioeng.*, **102**, 1 (2006); https://doi.org/10.1263/jbb.102.1
5. V. Bansal, P. Poddar, A. Ahmad and M. Sastry, *J. Am. Chem. Soc.*, **128**, 11958 (2006); https://doi.org/10.1021/ja063011m
6. M.S. Chavali and M.P. Nikolova, *SN Appl. Sci.*, **1**, 607 (2019); https://doi.org/10.1007/s42452-019-0592-3
7. M.E. Franke, T.J. Koplin and U. Simon, *Small*, **2**, 36 (2006); https://doi.org/10.1002/smll.200500261
8. A. Haider, M. Ijaz, S. Ali, J. Haider, M. Imran, H. Majeed, I. Shahzadi, M.M. Ali, J.A. Khan and M. Ikram, *Nanoscale Res. Lett.*, **15**, 50 (2020); https://doi.org/10.1186/s11671-020-3283-5
9. H. Abdul Salam, R. Sivaraj and R. Venckatesh, *Mater. Lett.*, **131**, 16 (2014); https://doi.org/10.1016/j.matlet.2014.05.033
10. K. Saoud, R. Alsoubaihi, N. Bensalah, T. Bora, M. Bertino and J. Dutta, *Mater. Res. Bull.*, **63**, 134 (2015); https://doi.org/10.1016/j.materresbull.2014.12.001
11. H. Agarwal, S. Venkat Kumar and S. Rajeshkumar, *Resour. Efficient Technol.*, **3**, 406 (2017); https://doi.org/10.1016/j.reffit.2017.03.002
12. F. Xu, Q. Qin, A. Mishra, Y. Gu and Y. Zhu, *Phys. Rev. Lett.*, **134**, 169 (2007); https://doi.org/10.1007/s12274-010-1030-4
13. A. Sulciute, K. Nishimura, E. Gilshtein, F. Cesano, G. Viscardi, A.G. Nasibulin, Y. Ohno and S. Rackauskas, *J. Phys. Chem. C*, **125**, 1472 (2021); https://doi.org/10.1021/acs.jpcc.0c08459
14. S. Raha and M. Ahmaruzzaman, *Nanoscale Adv.*, **4**, 1868 (2022); https://doi.org/10.1039/D1NA00880C
15. X. Wang, Y. Ding, C.J. Summers and Z.L. Wang, *J. Phys. Chem. B*, **108**, 8773 (2004); https://doi.org/10.1021/jp048482e
16. H. Mirzaei and M. Darroudi, *Ceram. Int.*, **43**, 907 (2017); https://doi.org/10.1016/j.ceramint.2016.10.051
17. M. Sundrarajan, S. Ambika and K. Bharathi, *Adv. Powder Technol.*, **26**, 1294 (2015); https://doi.org/10.1016/j.apt.2015.07.001
18. M. Anbuvannan, M. Ramesh, G. Viruthagiri, N. Shanmugam and N. Kannadasan, *Spectrochim. Acta A Mol. Biomol. Spectrosc.*, **143**, 304 (2015); https://doi.org/10.1016/j.saa.2015.01.124
19. A. Kolodziejczak-radzimska and T. Jesionowski, *Materials*, **7**, 2833 (2014); https://doi.org/10.3390/ma7042833

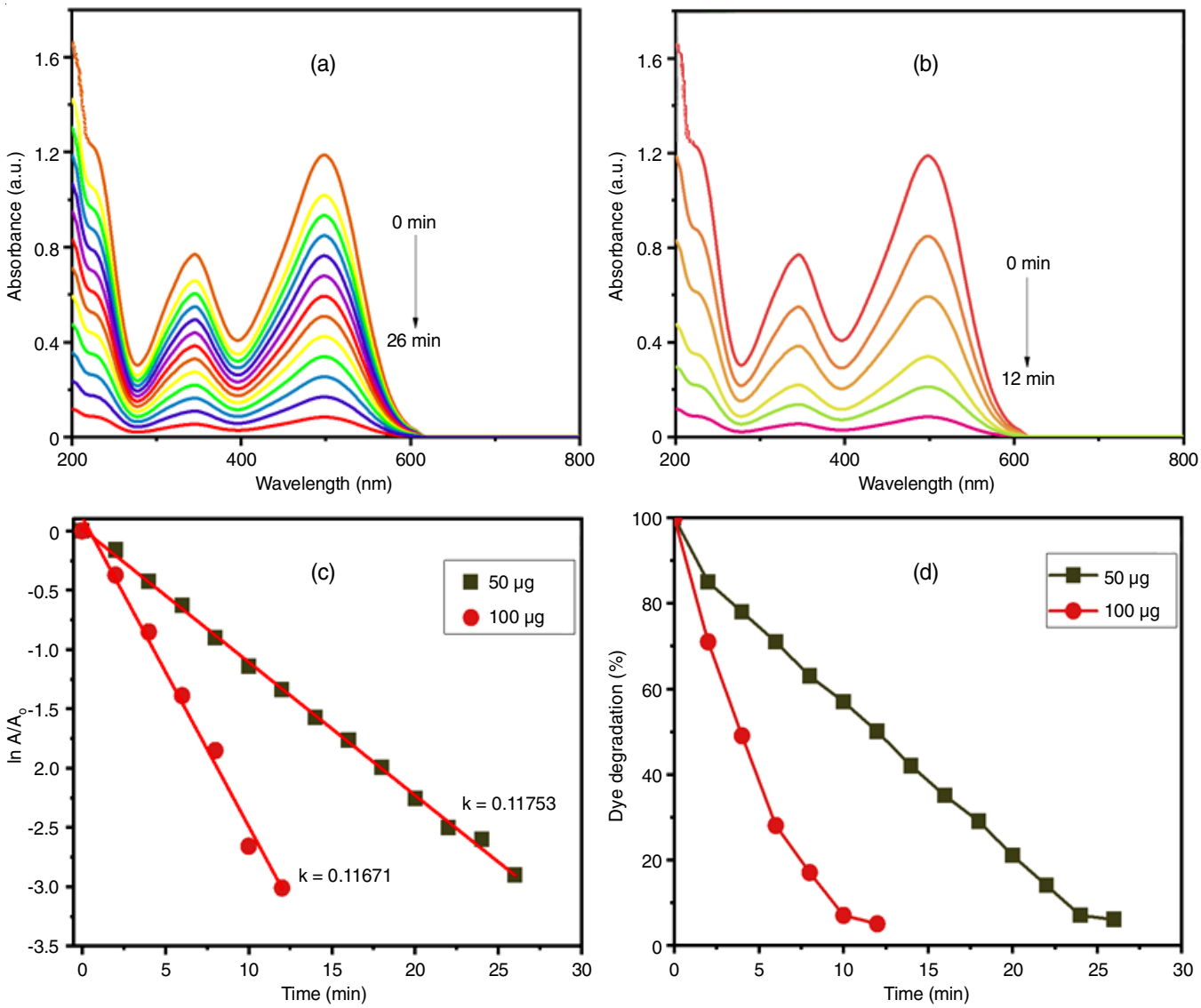

Fig. 6. Time-dependent UV-vis spectra for the catalytic degradation of Congo red dyes by $NaBH_4$ in the presence of ZnO nanoparticles as catalyst. Conditions: [$NaBH_4$] = 0.3 M; methylene blue = 0.1 mM; ZnO nanoparticles (50 and 100 µg)

20. D.B. Bharti and A.V. Bharati, *Luminescence*, **32**, 317 (2017); https://doi.org/10.1002/bio.3180
21. K.G. Akpomie, S. Ghosh, M. Gryzenhout and J. Conradie, *Sci. Rep.*, **11**, 8305 (2021); https://doi.org/10.1038/s41598-021-87819-2
22. J. Lu, K.M. Ng and S. Yang, *Ind. Eng. Chem. Res.*, **47**, 1095 (2008); https://doi.org/10.1021/ie071034j
23. E.D. Mohamed Isa, K. Shameli, N.W. Che Jusoh, S.N.A.M. Sukri and N.A. Ismail, *IOP Conf. Ser.: Mater. Sci. Eng.*, **1051**, 012079 (2021); https://doi.org/10.1088/1757-899X/1051/1/012079
24. M. Naseer, U. Aslam, B. Khalid and B. Chen, *Sci. Rep.*, **10**, 9055 (2020); https://doi.org/10.1038/s41598-020-65949-3
25. J. Qu, X. Yuan, X. Wang and P. Shao, *Environ. Pollut.*, **159**, 1783 (2011); https://doi.org/10.1016/j.envpol.2011.04.016
26. T.U. Doan Thi, T.T. Nguyen, Y.D. Thi, K.H. Ta Thi, B.T. Phan and K.N. Pham, *RSC Adv.*, **10**, 23899 (2020); https://doi.org/10.1039/D0RA04926C
27. D. Thatikayala, V. Banothu, J. Kim, D.S. Shin, S. Vijayalakshmi and J. Park, *J. Mater. Sci. Mater. Electron.*, **31**, 5324 (2020); https://doi.org/10.1007/s10854-020-03093-4
28. S.K. Urge, S.T. Dibaba and A.B. Gemta, *J. Nanomater.*, **7**, 7036247 (2023); https://doi.org/10.1155/2023/7036247
29. U.P. Singh, B. Prithiviraj, B.K. Sarma, M. Singh and A.B. Ray, *Indian J. Exp. Biol.*, **39**, 310 (2001).
30. S. Abel, J.L. Tesfaye and R. Shanmugam, *J. Nanomater.*, **2021**, 3413350 (2021); https://doi.org/10.1155/2021/3413350
31. H. Mofid, M.S. Sadjadi, M.H. Sadr, A. Banaei and N. Farhadyar, *Adv. Nano Chem.*, **2**, 32 (2020); https://doi.org/10.22126/ANC.2020.4745.1016
32. K. Elumalai and S. Velmurugan, *Appl. Surf. Sci.*, **345**, 329 (2015); https://doi.org/10.1016/j.apsusc.2015.03.176
33. H.Y. Chai, S.M. Lam and J.C. Sin, *AIP Conf. Proc.*, **2157**, 020042 (2019); https://doi.org/10.1063/1.5126577
34. S. Pal, K. Pal, S. Mukherjee, D. Bera, P. Karmakar and D. Sukhen, *Mater. Res. Express*, **7**, 015068 (2020); https://doi.org/10.1088/2053-1591/ab69c8
35. A. Jayachandran, A. T.R and A.S. Nair, *Biochem. Biophys. Rep.*, **26**, 100995 (2021); https://doi.org/10.1016/j.bbrep.2021.100995
36. P. Nagajyothi, S.J. Cha, I.J. Yang, T. Sreekanth, K.J. Kim and H.M. Shin, *J. Photochem. Photobiol. B*, **146**, 10 (2015); https://doi.org/10.1016/j.jphotobiol.2015.02.008

37. X. Cai, Y. Luo, W. Zhang, D. Du and Y. Lin, *ACS Appl. Mater. Interfaces*, **8**, 22442 (2016); https://doi.org/10.1021/acsami.6b04933
38. M. Alhujaily, S. Albukhaty, M. Yusuf, M.K.A. Mohammed, G.M. Sulaiman, H. Al-Karagoly, A.A. Alyamani, J. Albaqami and F.A. AlMalki, *Bioengineering*, **9**, 541 (2022); https://doi.org/10.3390/bioengineering9100541
39. A. Sirelkhatim, S. Mahmud, A. Seeni, N.H.M. Kaus, L.C. Ann, S.K.M. Bakhori, H. Hasan and D. Mohamad, *Nanomicro Lett.*, **7**, 219 (2015); https://doi.org/10.1007/s40820-015-0040-x
40. A. Ali , A.-R. Phull and M. Zia, *Nanotechnol. Rev.*, **7**, 413 (2018); https://doi.org/10.1515/ntrev-2018-0067
41. S.J.P. Begum, S. Pratibha, J.M. Rawat, D. Venugopal, P. Sahu, A. Gowda, K.A. Qureshi and M. Jaremko, *Pharmaceuticals*, **15**, 455 (2022); https://doi.org/10.3390/ph15040455
42. S. Alamdari, M. Sasani Ghamsari, G. Lee, W. Han, H.H. Park, M.J. Tafreshi, H. Afarideh and M.H.M. Ara, *Appl. Sci.*, **10**, 3620 (2020); https://doi.org/10.3390/app10103620
43. S. Faisal, H. Jan, S.A. Shah, S. Shah, A. Khan, M.T. Akbar, M. Rizwan, F. Jan, Wajidullah, N. Akhtar, A. Khattak and S. Syed, *ACS Omega*, **6**, 9709 (2021); https://doi.org/10.1021/acsomega.1c00310
44. J. Singh, T. Dutta, K.H. Kim, M. Rawat, P. Samddar and P. Kumar, *J. Nanobiotechnology*, **16**, 84 (2018); https://doi.org/10.1186/s12951-018-0408-4
45. Y. Yan, H. Yang, Z. Yi and T. Xian, *Catalysts*, **9**, 795 (2019); https://doi.org/10.3390/catal9100795